A Zabala *et al* 2020 *Surf. Topogr.: Metrol. Prop.* **8** 024001

DOI 10.1088/2051-672X/ab82a3

Development of a novel method to characterize mean surface peak curvature as a signature of tribological performance of dental implant surfaces

A. Zabala[1], L Blunt[2], A. Aginagalde[1], I. Llavori[1], W. Tato[1]

[1]Mondragon University, Surface Technologies Research Group
[2]University of Huddersfield, EPSRC Advanced Metrology Hub

E-mail: azabalae@mondragon.edu

Keywords: dental implant, implant integrity, surface topography, feature parameters, surface curvature

*Corresponding author: azabalae@mondragon.edu (Alaitz Zabala)

ABSTRACT

The integrity of dental implant surfaces might be compromised during surgical insertion. Wear and topographical modifications can occur during implant insertion, which can potentially have clinical implications. Accordingly, the analysis and prediction of the wear behaviour of dental implant surfaces is fundamental. Surface mean curvature is a key topographical parameter in contact mechanics, related to wear and plastic deformation; however, there is not a consensus on its characterization. In this paper, a critical analysis of the feature parameter S_{pc} from ISO 25178-2 is carried out, which addresses its limited ability to characterize dental implant surfaces. A novel alternative parameter (named 'relative mean peak curvature' ΔS_{dq}) is presented and evaluated in representative dental implant treatments. The obtained results suggest a positive correlation between the surface peak curvature and its tribological signature in biomedical implants. Although biomedical experiments are needed to validate this correlation, the novel method is presented as a tool for future studies.

KEYWORDS: dental implant, implant integrity, surface topography, feature parameters, peak curvature

1 Introduction

Titanium based dental implants has become the preferred choice for tooth replacements [1]. Among different strategies to increase the osseointegration [2], the surface modification of dental implants has become a common one in oral rehabilitation, since a rougher surface has been related to better bone apposition [3,4]. However, the high peaks of the roughened surfaces are potentially prone to breaking off and detaching during the surgical insertion into the bone structure. Recent studies have shown that the implant surfaces can be subjected to wear during insertion, leading to particle detachment [5–7]. The release of titanium particles to adjacent tissues has clinical implications; it has been related to increased bone resorption activity [8], the possibility of peri-implantitis [9–11], stronger pro-inflammatory response in macrophages [12], increased early bone loss [13] and, ultimately, implant failure [14]. Accordingly, the analysis and prediction of the wear behaviour of dental implant surfaces is fundamental in implant dentistry to improve the implant design, implantation protocols and performance of the implant.

It is widely accepted that rough surfaces usually wear more quickly than smooth surfaces [15]. However, the majority of models cannot account for differences in wear rates for surfaces with differing topographies operating in otherwise identical conditions. Meng and Ludema [16] have identified nearly 200 ‘wear equations’ that consider a wide variety of material properties and operating conditions. However, only 4 out of the 28 equations selected for further analysis considered topography-related parameters. In these equations, the mean peak curvature and the mean slope have been identified as important surface topography characteristics [17].

Greenwood and Williamson [18] defined a dimensionless parameter combining both material and topographical properties to determine if a contact would be elastic or plastic (the so-called ‘plasticity index’). In this model, the rough surface is covered with homogeneously distributed summits (density: η) that are spherical in shape (constant radius: β) and have a normal height distribution (standard deviation: σ). The plasticity index defined by Greenwood and Williamson is given by equation 1:

$$\psi_{\mathrm{GW}} = \frac{E'}{H}\sqrt{\frac{\sigma}{\beta}} \tag{1}$$

where the E'/H ratio is the material property ratio, H is the hardness and E′ corresponds to the reduced elastic modulus, which is derived from the material properties of the two contacting bodies, as described in equation 2:

$$\frac{1}{E'} = \frac{1-\nu_1^2}{E_1} + \frac{2-\nu_2^2}{E_2} \quad (2)$$

In this equation, ν is the Poisson coefficient and E is the elastic modulus.

Therefore, the approach developed above indicates that the contact behaviour of a surface can be described using both material and topographical parameters. Greenwood and Williamson emphasised that wear is much more prone in contacting plastic asperities than in elastic ones [19]. They were able to demonstrate that the highest percentiles of summits would deform at any load plastically for $\Psi_{GW} > 1$, elastically when $\Psi_{GW} < 0.6$ and would present different behaviours depending on the load in the range of $0.6 < \Psi_{GW} < 1$. Therefore, a low plasticity index is related to superior wear properties [20,21].

A different topographical parameter combination was later introduced by Greenwood and Tripp [22] (see equation 3) to describe topographical characteristics within a formulation to calculate the contact pressure of two nominally rough surfaces. This dimensionless product of summit properties (η: density, β: curvature radius, and σ: deviation of the height distribution) has been successfully correlated with wear [23].

$$\eta \cdot \beta \cdot \sigma \quad (3)$$

The revised models show that the peak curvature has a significant role in the wear performance; accordingly, its proper characterization is important. However, the definition of the peak curvature is still controversial. Greenwood himself concluded that 'The introduction by Greenwood and Williamson in 1966 of the definition of a "peak" as a point higher than its neighbours on a profile sampled at a finite sampling interval was, in retrospect, a mistake, although it is possible that it was a necessary mistake' [24]. As stated by Bashevskaya et al. [25], the identification of peak radii using a geometrical approach requires complex algorithms. The lack of standard methods to characterise peak curvature leads to significant differences in the published data. Tomanik et al. [26] have analysed different reports on piston rings' studies and concluded that the reported curvature radius (β) varied considerably (66-5,000 μm). It is to be presumed that the surfaces analysed in the studies may be different, although those differences appear to be too large if one considers that the surfaces have the same functionality. Regarding the possible reasons for those discrepancies it should be remembered at this point that different methods are available for the peak radius computation. Multiscale approaches

has been developed in order to characterize curvature properties at different scales [27,28], which requires to define the region where the curvature for each vertex is calculated. However, this research will focus in approaches to compute curvature of peaks on scale-limited surfaces for contact mechanic related functionalities.

Nayak and McCool [29] demonstrated that topographical parameters describing surface asperities may be computed or approximated using spectral moments (*m0, m2, m4*) calculated from a cross section [30]. These quantities, and the surface curvature radius would then be defined as follows:

$$\beta = 0.375\left(\frac{\pi}{m_4}\right)^{\frac{1}{2}} \tag{4}$$

Although this approach is extensively used (see, for instance, [31,32]) the value of the curvature radius (β) for different cross-sections extracted from the same surface may vary significantly [29]. This is why the second approach relies on average values of the spectral moments (obtained from various cross-sections of the 3D surface) to calculate the topographical parameters, therefore obtaining more reliable parameters (some examples in [33,34]). On the other hand, a third method of obtaining the topographical parameters is based on determining the asperities of the surface through the summit identification scheme. This approach calculates parameters directly on the summits (identified as local maxima); thus, it does not rely upon statistical methods [35]. Pawar et al. [36] have analysed the differences obtained when using approaches based on spectral moments and the summit identification scheme. They found that parameters vary considerably depending on the method used and highlighted the summit identification approach as the most reliable. It can be seen that although there is a consensus on the importance of the surface peak curvature in contact mechanics, there is not a consensus on its characterization.

This paper carries out a critical analysis of the feature parameter S_{pc} and proposes a new method to characterize the surface peak curvature as a descriptor for the analysis of the tribological performance of dental implant rough surfaces. The paper is structured as follows. In Section 2, the treatments of surfaces and the measurement conditions of the selected benchmark dental implant surfaces are described. In Section 3, a critical analysis of the suitability of the currently available feature parameter S_{pc} is carried out. In Section 4, after determining that the feature parameter is not suitable to properly describe the

surface curvature, a novel method and parameter is proposed. Lastly, Section 5 discusses the results in the context of applying the new parameter to real dental implant surfaces.

2 Surfaces under study and measurement conditions

Commercially pure titanium discs (Grade IV, diameter 6 mm, thickness 1 mm) with turned surfaces were used as an initial base line material. Typical dental implant surface treatments were selected for the study: acid etching, and sand blasting followed by acid etching. A total of four surface types were generated, with five samples for each type: (i) non-treated as machined surface (MCN); (ii-iii) two degrees of acid etching treatments, (AE1 and AE2) and (iv) sand blasting followed by acid etching treatment (SB+AE), see Figure 1.

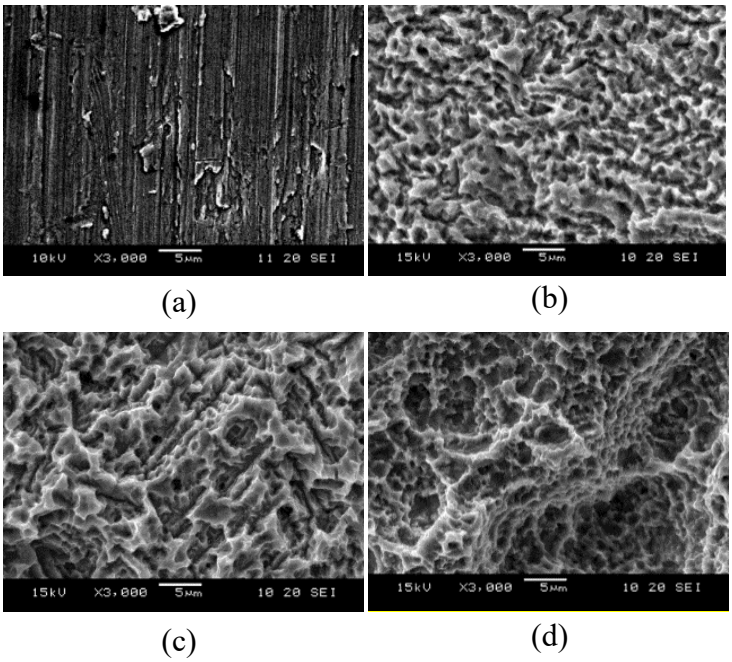

Figure 1: SEM images of the four surface treatments under study: (a) as machined (MCN), (b) acid-etched 1 (AE1), (c) acid-etched 2 (AE2), (d) sand-blasted and acid-etched (SB+AE).

Quantitative characterization of the surfaces was performed by a confocal profilometer (Plμ-SENSOFAR) with objective 100xSLWD (Super Long Working Distance, NA=0.9, spatial sampling 0.18 μm). Four measurements with a surface area of 250x187 μm^2 were acquired for each sample (a total of 20 measurements per each surface type). The metrological software SensoMap Turbo 5.1 (Digital Surf) was used for data post-

processing. A Gaussian S filter of 0.36x0.36 μm^2 was applied for noise elimination, and a plane fitting was used as form operator. Further analysis (explained in the following sections) was performed in the scale-limited primary SF surfaces.

3 Feature parameters evaluation and critical study

In this section, the suitability of the feature parameter S_{pc} (arithmetic mean peak curvature) as a way to characterize the mean surface peak curvature is analysed. Unlike field parameters, in which all the points on the surface are considered in the calculation, feature parameters consider only the pre-identified features on the surface. Therefore, characteristics of specific features can be characterized on scale-limited surfaces, following the five steps defined in ISO 25178-2 [37]: (i) selection of the type of texture feature, (ii) segmentation, (iii) determination of the significant features, (iv) selection of feature attributes and (v) quantification of feature attribute statistics.

Feature parameters only consider significant features, eliminating insignificant motifs using the Wolf pruning approach, which combines adjacent peaks or pits with the smallest height difference until a pre-defended threshold is reached [37]. Figure 2 shows two of the surfaces under analysis (SB+AE and AE2) both before and after the pruning process. Before the pruning, the surfaces are over-segmented into a large number of non-significant small features. By simple visual examination of the figures, it is clear that after pruning only the significant peaks are retained.

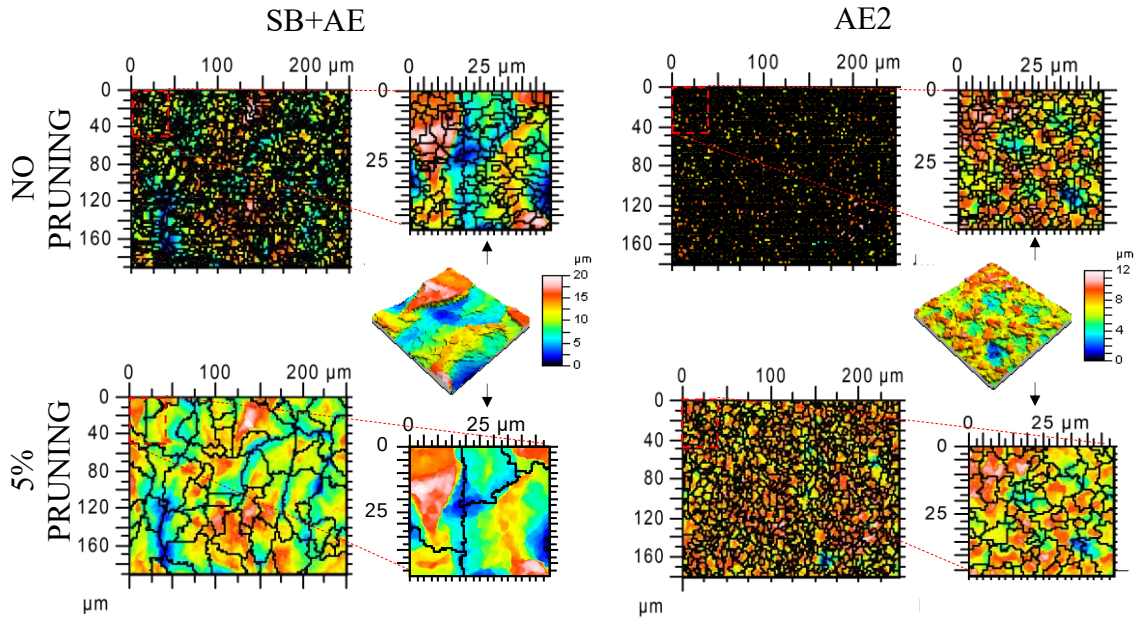

Figure 2: Analysis of the Wolf pruning effect (under standard conditions: 5% of S_z, [37]) on two of the surface treatments under study, SB+AE and AE2.

A full description of the feature determination process can be found in the literature [38]. The following is an analysis of the feature parameter S_{pc} as a potential candidate to describe the mean peak radius of dental implant surfaces.

The arithmetic mean curvature of significant peaks (which is the reciprocal of the peak radius, i.e., $S_{pc} = 1/\beta$) is given in [1/µm]. The S_{pc} value of the surfaces under analysis was calculated using the metrological software SensoMap Turbo 5.1 (Digital Surf) under standard conditions (pruning= 5% of S_z, [37]). Figure 3 (a) shows the obtained results.

The arithmetic mean curvature values present a ranking in increasing order as follows: MCN, AE1, AE2, SB+AE2. SB+AE has the biggest S_{pc} value, and therefore the biggest curvature, while the MCN surface has the lowest S_{pc} value, and therefore the most rounded peaks. Both acid-etched treatments (AE1, AE2) have intermediate values, although AE1 is significantly smaller.

Analysing the significant features in Figure 3(b), it can be clearly seen that the SB+AE treatment generates less sharp peaks as compared to etched surfaces (AE1, AE2), and should therefore present a smaller curvature value. Machined surface (MCN) has a smooth non-isotropic surface.

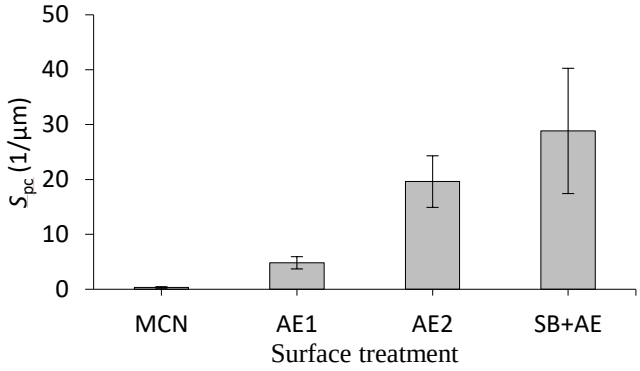

(a)

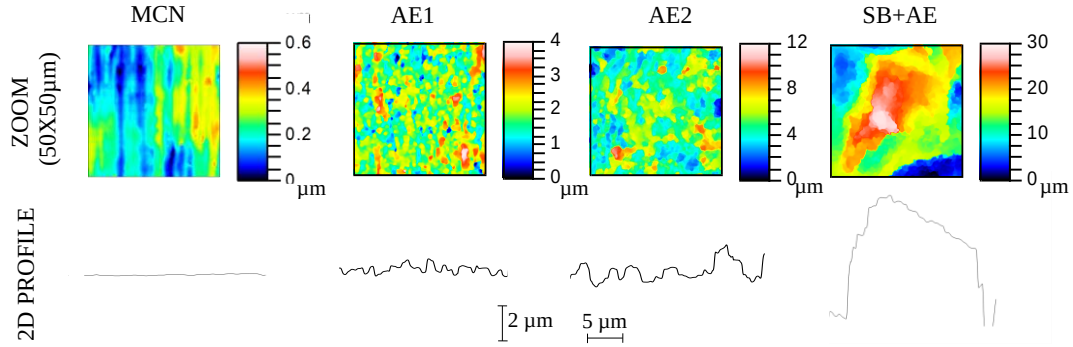

(b)

Figure 3: Quantitative and qualitative analysis of the peak curvature of the surfaces studied. (a) Results of the feature parameter S_{pc}. (b) Representative zoom images (free scale) and profiles (imposed scale) of the four surface treatments under study.

It follows from this that the peak curvature parameter S_{pc} does not accurately represent the significant feature characteristics (since the SB+AE treatment had the greatest S_{pc} value). In accordance with the present results, the instability of the S_{pc} parameter had been previously reported by Wang et al. [39], and was attributed to the overestimation of the noise peak points.

It should be emphasised at this point that, once the surface is segmented, the method by which the curvature should be calculated is not specified unambiguously in the ISO 25178-2 standard [37]. Its ancestor (the summit curvature, S_{sc}) is not strictly defined in the standard, although it was established earlier in the research [40], which contributed to ISO 25178-2 as follows:

$$S_{sc} = -\frac{1}{2}\frac{1}{n}\left(\sum_{k=1}^{n} \frac{\partial \eta^2(x,y)}{\partial x^2}\frac{+\partial \eta^2(x,y)}{\partial y^2}\right) \quad (5)$$

where η is the mean value surface (the reference datum) and n is the number of summits. The main difference between the old (S_{sc}) and new (S_{pc}) parameters is that for the latter parameter (S_{pc}), only significant peaks are taken into account, due to the pruning of the change tree [38]. However, there are different ways to compute the arithmetic peak curvature once the peaks have been segmented. The simplest way is to calculate the arithmetic mean summit curvature based on three data points in each direction, while other approaches take into account up to seven data points in each direction [41]. In this respect, Digital Surf software does not provide information regarding the curvature determination method.

It is to be presumed that the method used to estimate the curvature may considerably affect the obtained value, since actual surfaces are not perfect spheres. It is likely that this was the source of the discrepancies encountered and one of the limitations of the parameter (see Figure 4).

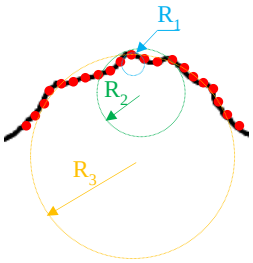

Curvature calculating method based on	Normalised radius	Normalised curvature
Three data points	R_1=1	S_{pc}=1
Seven data points	R_2=6	S_{pc}=0.17
Whole peak	R_3=13	S_{pc}=0.077

Figure 4: Illustrative representation of the effect of the curvature calculating method on the peak radius and curvature estimation.

It is therefore concluded that the feature parameter S_{pc} is not able to properly characterize the surface mean curvature in the present case. The following section presents the novel method developed for surface peak mean curvature characterization pertaining to the present surfaces.

4 Novel method for curvature determination

Rationale

The rationale behind the approach outlined in this study is that the mean slope of the surface, as a function of height, changes more rapidly in surfaces with sharp peaks as compared to those with rounded peaks (see Figure 5).

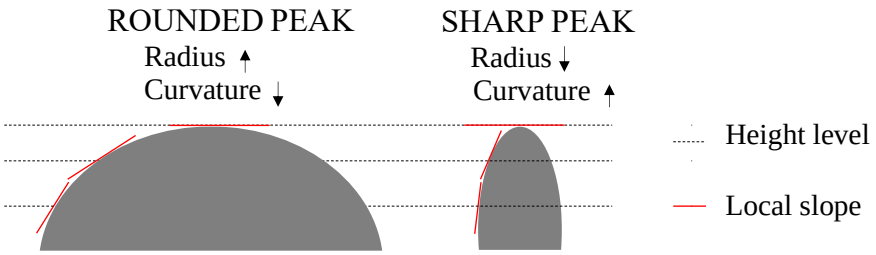

Figure 5: Illustrative representation of the evolution of the local slope as a function of height for a rounded (left) and a sharp (right) peaks.

Based on the fact that the S_{dq} parameter [37] represents the root mean square slope of the surface, a novel method based on S_{dq} has been developed to yield a representative parameter of mean peak curvature.

First, the evolution of the S_{dq} parameter as a function of height is calculated through an iterative process programmed in Matlab®. The primary surface is truncated at different heights, and the S_{dq} value of the remaining surface is calculated for each truncation level. As shown in Figure 6, the process starts from the highest point on the surface (h_{tr} =0) and the truncation height (h_{tr}) is augmented progressively by a constant step size (step$_{tr}$) until it reaches the total surface height ($h_{tr} = S_z$; the effect and selection of the truncation step size [step$_{tr}$] is discussed in later sections). In this way, an evolution curve of the S_{dq} as a function of truncation height (h_{tr}) is obtained (this curve is S-shaped).

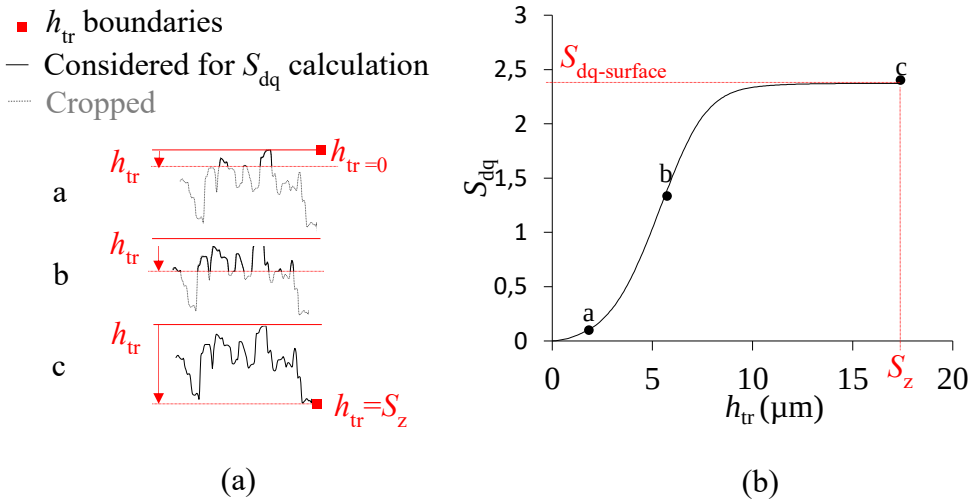

Figure 6: Evolution of S_{dq} as a function of the truncation height (h_{tr}). (a) Schematic illustration of the method: increasing truncation levels are applied and the S_{dq} value is calculated at each remaining upper surface. (b) Representative graph of the S_{dq} evolution curve as a function of the truncation height.

To demonstrate the relationship between the evolution of the surface mean slope (S_{dq}) as a function of truncation height (h_{tr}) and the consequent mean peak curvature, a series of

surfaces with decreasing peak curvatures were generated using filtering. Figure 7 shows the S_{dq} evolution curve of an acid-etched (AE1) primary (SF) and waviness (LF) surfaces of two different cut-off values (which have lower mean curvatures than the primary surface does). It can be clearly seen that there is a linear section of the slopes (the slope of the linear section will be named ΔS_{dq}). The slope value decreases as the curvature decreases; therefore, the ΔS_{dq} parameter can be used intuitively to indicate the mean peak curvature of a surface in relative terms (the larger the slope, the greater the curvature). The following sections describe the methodology used to calculate this slope (ΔS_{dq}) in an efficient and reproducible way.

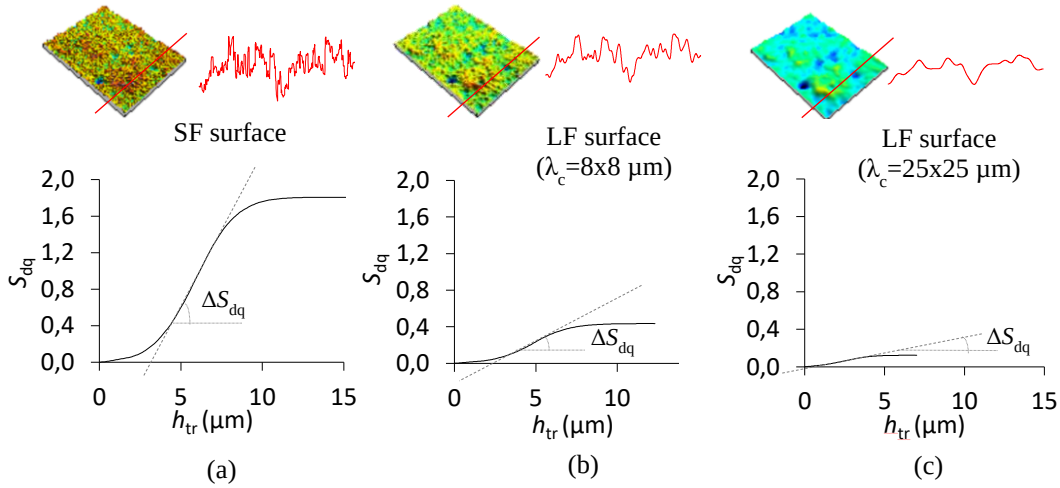

Figure 7: Demonstration of the relationship between the evolution of the S_{dq} as a function of truncation height (h_{tr}) and the surface mean curvature (characterized through the curve slope, ΔS_{dq}). Different mean curvatures were simulated through filtering, in decreasing order: (a) AE1 primary (SF) surface; (b) AE1 waviness (LF) surface (Lfilter: Gaussian filter λ_c= 8x8 um), (c) AE1 waviness (LF) surface (L filter: Gaussian filter λ_c = 25x25 um).

Proposed novel parameter: relative mean peak curvature, ΔS_{dq}

As discussed in the previous sections, the growing rate of the S_{dq} evolution curve (ΔS_{dq}; Figure 7) is representative of the relative mean surface curvature. The following describes the method proposed to calculate the novel ΔS_{dq} parameter (the slope of the S_{dq} evolution curve) in a reproducible way.

Firstly, the numerical approximation of the first derivative of the evolution curve is calculated using the 'diff' function in Matlab, applying the resolution of the curve ($step_{tr}$) as step size (see Figure 8). Due to the S-shape of the curve, the derivative curve has a bell shape, since the trend changes from upward to downward when the original turns from

convex to concave. Therefore, the abscissa of the maximum point at the derivative graph (p) corresponds to the position of the intersection point of the original curve. Additionally, by definition, the value of the first derivative at 'p' point corresponds to the slope of the tangent line to the original graph at the inflexion point, which is the targeted slope.
Thus, the ΔS_{dq} is easily obtained by calculating the first derivative of the S_{dq} evolution graph and finding the maximum value.

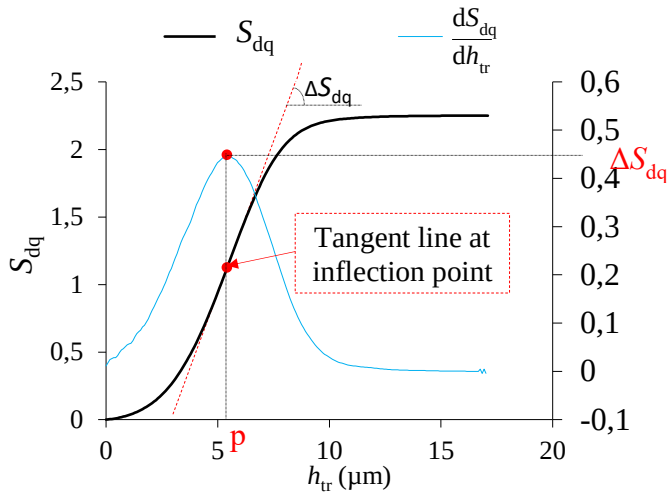

Figure 8: Illustration of the ΔS_{dq} calculation. The first derivative of the S_{dq} evolution curve is calculated (h_{tr}= truncation height). The maximum point of the S_{dq} derivative is the slope of the tangential line of the evolution curve at the inflexion point = ΔS_{dq}.

Selection of optimum truncation step size

It should be considered that the S_{dq} evolution curve will be sensitive to the truncation step size ($step_{tr}$), and therefore the slope value (ΔS_{dq}) may vary. Figure 9 displays the slope value (ΔS_{dq}) and calculation times obtained for different truncation step sizes ($step_{tr}$) that correspond to the surface that presents the biggest S_z value (SB+AE).

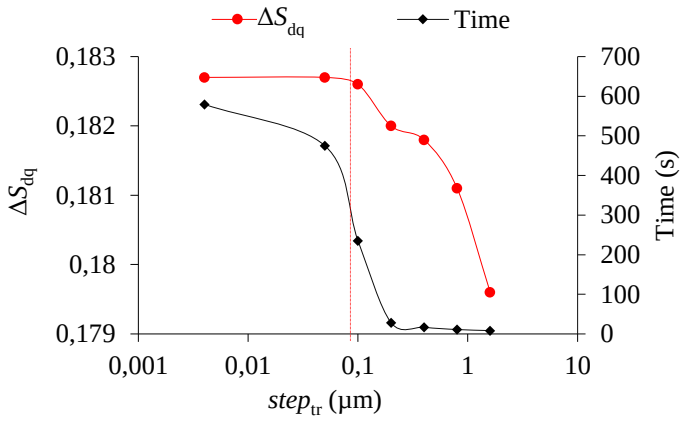

Figure 9: Effect of the truncation step size ($step_{tr}$) on the ΔS_{dq} value and calculation time. Values of the sensitivity study (a), and graphical representation (b).

The calculation time decreased exponentially when the step size was increased, until it reached a stable trend (for $step_{tr}$ values greater than 0.2 µm). This had been anticipated because the $step_{tr}$ value determines the resolution of the curve and will therefore be directly related to the calculation time. The slope (ΔS_{dq}) value remained fairly stable until a $step_{tr}$ size of 0.1 µm, after which it decreased considerably. A compromise between reliability and calculation time was sought by selecting a $step_{tr}$ of 0.1 µm (corresponding to 367 steps) as the optimum value. The step size of each surface was therefore calculated as follows:

$$h_{\mathrm{tr}} = \frac{S_z}{367} \tag{6}$$

5 Results and discussion

Using the previously explained method, the proposed ΔS_{dq} parameter that describes the relative surface peak curvature was calculated for representative dental implant surfaces (introduced in section 2). Figure 10 depicts representative S_{dq} evolution curves (a) and the mean results of ΔS_{dq} values (b) calculated from 20 measurements for each surface type under consideration.

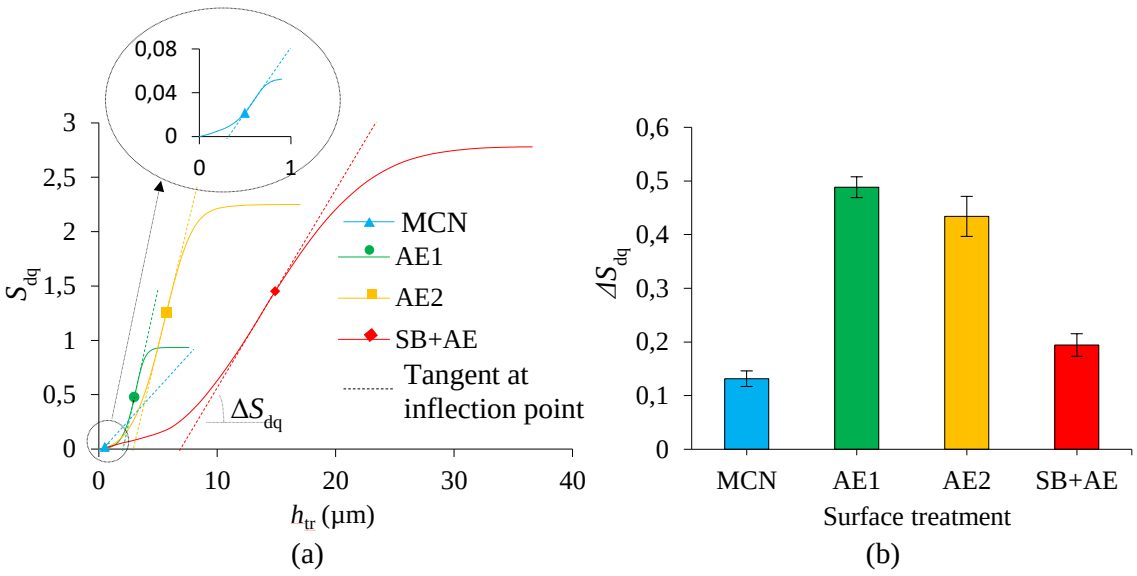

Figure 10: Results of the ΔS_{dq} parameter for the four surface types under analysis: (a) Representative curves of the S_{dq} evolution as a function of truncation height (h_{tr}) from which the ΔS_{dq} value is calculated. (b) Results of the ΔS_{dq} value for the four surface types under analysis.

The ΔS_{dq} parameter presented stable values (coefficients of variation lower than 11%), demonstrating that it is a robust parameter. In contrast to the S_{pc} parameter (analysed in Section 3) and as seen in the surfaces of Figure 4, the ΔS_{dq} parameter represented the relative surface curvature properties. The surfaces can be ranked according to curvature from smallest to greatest as follows: MCN, SB+AE, AE2 and AE1.

As demonstrated by Greenwood and Williamson [18], wear is much more probable in asperities where plastic contact dominates (presenting smaller mean surface peak radius, $\beta \sim 1/\Delta S_{dq}$), than where elastic deformation is prominent. Therefore, a bigger surface mean curvature will increase the probability of particles detaching during dental implant insertion. Based on the obtained results, it can be inferred that the acid-etched surfaces would be more prone to wear, followed by the sand-blasted and acid-etched surfaces and, finally, the machined surface. This is in a good accordance previous works showing that the sand-blasted and acid-etched surface released lower quantities of titanium as compared to the acid-etched surfaces examined post insertion into the bone [42,43]. A lower trend to release particles of the machined surfaces compared to other roughened surfaces has also been reported [6,44].

Literature is scarce in studies on the wear response of dental implants after insertion. Accordingly, more biomedical tests would be needed in the future to fully validate the correlation between the surface peak curvature and its tribological signature in biomedical

implants. Due to the complexity of the multivariable interactions of the surface modification process (including implant macro geometry, surgical procedure and surface treatment), the follow-up work should be focused on studying the topographical modification behaviour in simplified shape samples subjected to simulated insertion forces. Based on the current results, it is anticipated that the surface mean curvature would play an important role in the correlation between 3D topographical parameters and the modification of dental implant surfaces generated during insertion. The present work exposes the limitations of the currently available feature parameter S_{pc} and proposes an alternative novel parameter, 'relative mean peak curvature' ΔS_{dq} to compute the curvature characteristic relevant in contact mechanics on the scale-limited surfaces.

It is not the aim of the authors to contribute to the so-called 'parameter rash' described by Whitehouse [45]; therefore, it should be noted that the presented parameter is a version of the already-standardized S_{dq} parameter [37] and is, in essence, a development of the toolbox ethos.

6 Conclusion

This paper critically analyses the standardized feature parameter S_{pc} and proposes a new parameter to characterize the relative surface peak curvature as a descriptor for the analysis of the tribological performance of dental implant rough surfaces during surgical insertion.

The new parameter (termed 'relative mean peak curvature', ΔS_{dq}) is a version of the already standardized S_{dq} parameter and is a development of the toolbox ethos.

Although biomedical experiments are needed to fully validate the correlation between the surface peak curvature and its tribological signature in biomedical implants, the obtained results suggests a positive correlation and is presented as a tool for future studies.

7 Acknowledgments

The authors gratefully acknowledge the financial support given by the Basque Government under the "Red guipuzcoana de Ciencia, Tecnología e Innovación" (Project BIOPREDICT: Ref.52/15, Project MOTOMODEL: Ref. OF 188/2017). L Blunt would like to gratefully acknowledge the UK's Engineering and Physical Sciences Research Council (EPSRC) funding of the Future Metrology Hub (Grant Ref: EP/P006930/1).

8 References

[1] Elani H W, Starr J R, Da Silva J D and Gallucci G O 2018 Trends in Dental Implant Use in the U.S., 1999–2016, and Projections to 2026 *J Dent Res* **97** 1424–30

[2] Albrektsson T Osseointegrated Titanium Implants: Requirements for Ensuring a Long-Lasting, Direct Bone-to-Implant Anchorage in Man 16

[3] Coelho P G, Granato R, Marin C, Teixeira H S, Suzuki M, Valverde G B, Janal M N, Lilin T and Bonfante E A 2011 The effect of different implant macrogeometries and surface treatment in early biomechanical fixation: An experimental study in dogs *Journal of the Mechanical Behavior of Biomedical Materials* **4** 1974–81

[4] Wennerberg A and Albrektsson T 2009 Effects of titanium surface topography on bone integration: a systematic review *Clinical Oral Implants Research* **20** 172–84

[5] Streckbein P, Wilbrand J-F, Kähling C, Pons-Kühnemann J, Rehmann P, Wöstmann B, Howaldt H-P and Möhlhenrich S C 2019 Evaluation of the surface damage of dental implants caused by different surgical protocols: an in vitro study *International Journal of Oral and Maxillofacial Surgery* **48** 971–81

[6] Pettersson M, Pettersson J, Molin Thorén M and Johansson A 2017 Release of titanium after insertion of dental implants with different surface characteristics – an *ex vivo* animal study *Acta Biomaterialia Odontologica Scandinavica* **3** 63–73

[7] Salerno M, Itri A, Frezzato M and Rebaudi A 2015 Surface Microstructure of Dental Implants Before and After Insertion: An In Vitro Study by Means of Scanning Probe Microscopy *Implant Dentistry* 1

[8] Oliveira N C M, Moura C C G, Zanetta-Barbosa D, Mendonça D B S, Cooper L, Mendonça G and Dechichi P 2013 Effects of titanium surface anodization with CaP incorporation on human osteoblastic response *Materials Science and Engineering: C* **33** 1958–62

[9] Fretwurst T, Nelson K, Tarnow D P, Wang H-L and Giannobile W V 2018 Is Metal Particle Release Associated with Peri-implant Bone Destruction? An Emerging Concept *J Dent Res* **97** 259–65

[10] Noronha Oliveira M, Schunemann W V H, Mathew M T, Henriques B, Magini R S, Teughels W and Souza J C M 2018 Can degradation products released from dental implants affect peri-implant tissues? *J Periodont Res* **53** 1–11

[11] Tawse-Smith A, Atieh M A, Leichter J, Girvan L and Rich A M 2015 Peri-Implant Bone Loss and Its Uncommon Causes: A Case Report *Clinical Advances in Periodontics* **5** 242–7

[12] Dodo C G, Meirelles L, Aviles-Reyes A, Ruiz K G S, Abranches J and Cury A A D B 2017 Pro-inflammatory Analysis of Macrophages in Contact with Titanium Particles and Porphyromonas gingivalis *Braz. Dent. J.* **28** 428–34

[13] Naveau A, Shinmyouzu K, Moore C, Avivi-Arber L, Jokerst J and Koka S 2019 Etiology and Measurement of Peri-Implant Crestal Bone Loss (CBL) *JCM* **8** 166

[14] Bölükbaşı N and Mercan S 2013 DETER MINATION OF TITANIUM PARTICLES AROUND A FAILED DENTAL IMPLANT *Vo l.* 6

[15] Blau P J 2009 *Friction science and technology: from concepts to applications* (Boca Raton, FL: CRC Press)

[16] Meng H C and Ludema K C Wear models and predictive equations: their form and content 15

[17] Thomas T R 1972 Computer simulation of wear *Wear* **22** 83–90

[18] Greenwood J A, Williamson J B P and Bowden F P 1966 Contact of nominally flat surfaces *Proceedings of the Royal Society of London. Series A. Mathematical and Physical Sciences* **295** 300–19

[19] Colaço R 2007 Surface-Damage Mechanisms: from Nano- and Microcontacts to Wear of Materials *Fundamentals of Friction and Wear* NanoScience and Technology ed E Gnecco and E Meyer (Berlin, Heidelberg: Springer) pp 453–80

[20] Torres B, Garrido M A, Rico A, Rodrigo P, Campo M and Rams J 2010 Wear behaviour of thermal spray Al/SiCp coatings *Wear* **268** 828–36

[21] Rosén B-G and Thomas T R 2001 Relationship of the plasticity index to machining parameters *International Journal of Machine Tools and Manufacture* **41** 2061–9

[22] Greenwood J A and Tripp J H 1970 The Contact of Two Nominally Flat Rough Surfaces *Proceedings of the Institution of Mechanical Engineers* **185** 625–33

[23] Anon 2003 *Advanced Techniques for Assessment Surface Topography* (Elsevier)

[24] Greenwood J A and Wu J J 2001 Surface Roughness and Contact: An Apology *Meccanica* **36** 617–30

[25] Bashevskaya O S, Bushuev S V, Nikitin A A, Romash E V and Poduraev Yu V 2017 Assessment of Surface Roughness Using Curvature Parameters of Peaks and Valleys of the Profile *Meas Tech* **60** 128–33

[26] Tomanik E, Chacon H and Teixeira G 2003 A simple numerical procedure to calculate the input data of Greenwood-Williamson model of asperity contact for actual engineering surfaces *Tribology Series* vol 41 (Elsevier) pp 205–15

[27] Maleki I, Wolski M, Woloszynski T, Podsiadlo P and Stachowiak G 2019 A Comparison of Multiscale Surface Curvature Characterization Methods for Tribological Surfaces *Tribology Online* **14** 8–17

[28] Bartkowiak T and Brown C A 2019 Multiscale 3D Curvature Analysis of Processed Surface Textures of Aluminum Alloy 6061 T6 *Materials* **12** 257

[29] McCool J I 1987 Relating Profile Instrument Measurements to the Functional Performance of Rough Surfaces *J. Tribol.* **109** 264

[30] Greenwood J A 2013 Contact of Rough Surfaces: The Greenwood and Williamson/Tripp, Fuller and Tabor Theories *Encyclopedia of Tribology* ed Q J Wang and Y-W Chung (Boston, MA: Springer US) pp 517–22

[31] Paggi M and Ciavarella M 2010 The coefficient of proportionality κ between real contact area and load, with new asperity models *Wear* **268** 1020–9

[32] Lee C-H, Eriten M and Polycarpou A A 2010 Application of Elastic-Plastic Static Friction Models to Rough Surfaces With Asymmetric Asperity Distribution *J. Tribol.* **132** 031602

[33] Ibrahim Dickey R D, Jackson R L and Flowers G T 2011 Measurements of the Static Friction Coefficient Between Tin Surfaces and Comparison to a Theoretical Model *J. Tribol.* **133** 031408

[34] Jackson R L and Green I 2011 On the Modeling of Elastic Contact between Rough Surfaces *Tribology Transactions* **54** 300–14

[35] Blanc J, Grime D and Blateyron F 2011 Surface characterization based upon significant topographic features *J. Phys.: Conf. Ser.* **311** 012014

[36] Pawar G, Pawlus P, Etsion I and Raeymaekers B 2012 The Effect of Determining Topography Parameters on Analyzing Elastic Contact Between Isotropic Rough Surfaces *J. Tribol* **135** 011401

[37] ISO 25178-2:2012 Geometrical product specifications (GPS) -- Surface texture: Areal -- Part 2: Terms, definitions and surface texture parameters, 2012.

[38] Blateyron F 2013 The Areal Feature Parameters *Characterisation of Areal Surface Texture* ed R Leach (Berlin, Heidelberg: Springer) pp 45–65

[39] Wang J, Jiang X, Gurdak E, Scott P, Leach R, Tomlins P and Blunt L 2011 Numerical characterisation of biomedical titanium surface texture using novel feature parameters *Wear* **271** 1059–65

[40] Anon Development of Methods for Characterisation of Roughness in Three Dimensions - 1st Edition

[41] Dong W P, Sullivan P J and Stout K J Comprehensive study of parameters for characterising three- dimensional surface topography IV: Parameters for characterising spatial and hybrid properties 16

[42] Zabala A, Blunt L, Tejero R, Llavori I, Aginagalde A and Tato W 2020 Quantification of dental implant surface wear and topographical modification generated during insertion *Surf. Topogr.: Metrol. Prop.* **8** 015002

[43] Sridhar S, Wilson T G, Valderrama P, Watkins-Curry P, Chan J Y and Rodrigues D C 2016 In Vitro Evaluation of Titanium Exfoliation During Simulated Surgical Insertion of Dental Implants *Journal of Oral Implantology* **42** 34–40

[44] Meyer U, Buhner M, Buchter A, Kruse-Losler B, Stamm T and Wiesmann H P 2006 Fast element mapping of titanium wear around implants of different surface structures *Clin Oral Implants Res* **17** 206–11

[45] Whitehouse D J 1982 The parameter rash — is there a cure? *Wear* **83** 75–8